

Neutron emission in Ni-H systems

A. BATTAGLIA^{(1)†}, L. DADDI⁽²⁾, S. FOCARDI⁽³⁾, V. GABBANI⁽⁴⁾, V. MONTALBANO⁽⁴⁾
F. PIANTELLI⁽⁴⁾, P. G. SONA⁽¹⁾ and S. VERONESI⁽⁴⁾

⁽¹⁾ *CISE spa, Segrate (MI) - Via Reggio Emilia 39, Milano, Italy*

⁽²⁾ *Accademia Navale di Livorno - Livorno, Italy*

⁽³⁾ *Dipartimento di Fisica, Università di Bologna e INFN sezione di Bologna
Bologna, Italy*

⁽⁴⁾ *Dipartimento di Fisica, Università di Siena e centro IMO - Siena, Italy*

(ricevuto il 9 Marzo 1996; revisionato il 14 Maggio 1999; approvato l'8 Settembre 1999)

*This paper is dedicated to the memory
of Adriano Battaglia*

Summary. — In this paper evidence is reported for neutron emission during energy production in Ni-H systems at about 700 kelvin. Neutrons were detected directly by He³ counters and indirectly by gold activation.

PACS 25.70.Ji – Fusion and fusion-fission reactions.

1. – Introduction

In a previous paper [1], the absence of penetrating radiation, during processes of anomalous heat production, was reported. Such a result was based on measurements performed, for safety reasons, by using dosimetric instrumentation and by comparing the radiation level near and far from a working cell.

Successively, such a cell (cell A) was modified and a new cell built (cell B). Both cells allow the measurement of their external wall temperature in order to detect any anomalous heat emission from the system. The calorimetric measurements have been presented and discussed elsewhere [2].

In particular, cell A produced a mean power of ≈ 38 W for 278 days and cell B produced ≈ 22 W for 319 days.

Since chemical reactions are ruled out for explaining such an energy release from the cells, a more accurate search for emission of radiation from the Ni-H system in the *excited*

† Deceased.

TABLE I. – *Characteristics of the neutron detectors used in the experiment.*

		<i>C1</i>	<i>C2</i>	<i>C3</i>
Detectors	Number of counters	1	2	1
	Count. mod. LND-INC	25325	25275	25275
	Counter diameter (mm)	50.8	25.4	25.4
	Counter length (mm)	387.4	342.9	342.9
	³ He pressure (Torr)	3040	7600	7600
Moderator	Material	paraffin	polithene	paraffin
	External dimensions (cm)	22 × 22 × 35	14.5 × 12 × 35	9.5 (diam.) × 33
Electronic and pulse processing	H.V. power SILENA	7716	7716	7716
	Preamplifier SILENA	205	2 × 205	205
	Lin. ampl. TENNELEC	TC205	TC205	TC205
	MCS analyzer SILENA	CICERO	CICERO	CATO
Abs. efficiency	8.4×10^{-6}	8.5×10^{-6}	7.4×10^{-6}	

state ⁽¹⁾ was undertaken. This research was based on the hypothesis that the calorimetric effects described in ref. [2] are the consequence of some kind of nuclear process. Our systems are able to remain in steady-state conditions for long time periods, allowing for a collection of statistically significant data. All neutron measurements reported in this paper were obtained for cell A (see fig. 1a in ref. [2]) which showed a greater heat excess.

Two methods were used for neutron detection: direct counting by means of neutron detectors and counting of γ -rays emitted by neutron activated gold [3]. Let us remark that the goal of the experiment described in this paper is to prove neutron emission in Ni-H systems. Because of the oneness of the experiment, the contemporaneity of the measurements performed in the two methods is only partial. Work is in progress for further quantitative measurements which are beyond the purposes of this paper.

2. – Direct neutron detection

Three ³He neutron detectors which will be identified as *C1*, *C2* and *C3* and whose characteristics are given in table I were employed. Each detector had its own power supply and amplification stages. In order to thermalize the incident neutrons, all counters were wound with moderators. The detector *C2* was made of two counters placed in the same moderator box. In order to reduce the thermal neutron background, a cadmium shield (1 mm thick) was placed around the *C1* and *C2* moderator and only afterwards also around the *C3* moderator. Thus, our detection system is able to reveal essentially neutrons whose energy is greater than the thermal one.

Figure 1a) shows a typical counter (unshielded) pulse spectrum amplitude, obtained with an Am-Be source of 2.2×10^5 neutrons/s strength, placed into a moderator in order to reduce the counting rate (usually the source was properly stocked in a building far from the laboratory where it was transferred only for the short calibration periods). The

⁽¹⁾ A calorimetric definition of *excited state* is given in ref. [2]. Practically, a Ni-H system in an *excited state* produces energy.

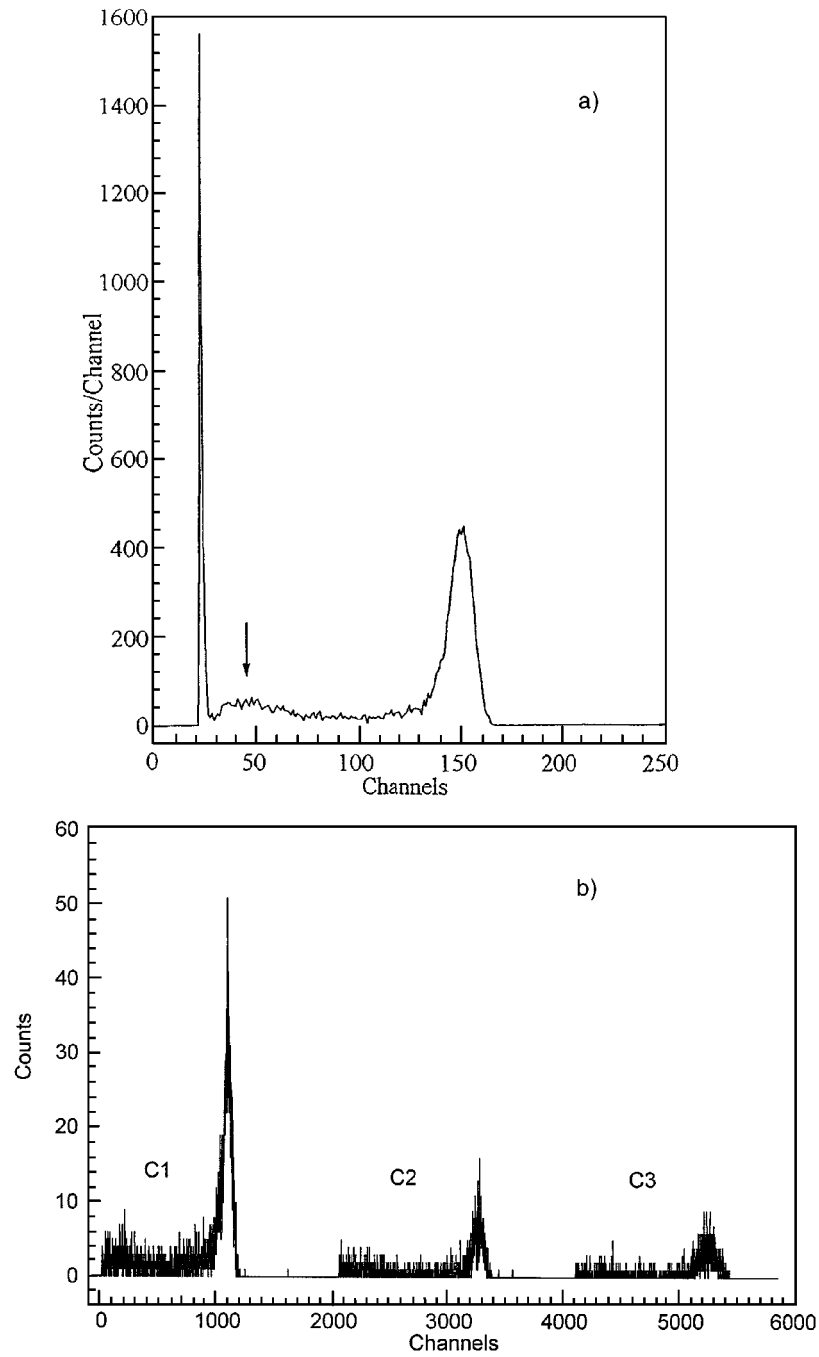


Fig. 1. – a) Amplitude spectrum obtained on utilizing detector *C2* and an Am-Be neutron source. The arrow indicates the electronic threshold chosen for measurements. b) Amplitude spectra of detectors *C1*, *C2* and *C3* placed near the cell in the measurement configuration. The three spectra were obtained with the same MCA in multichannel mode (2000 channels for every detector). The three peaks correspond in the new scale to the right peak shown in a).

spectrum shows, from the left: the gamma-rays' narrow peak, a broad band [4] due to the wall effect and the protons' peak generated in the ${}^3\text{He}(n, p){}^3\text{H}$ reaction. In order to reduce the gamma-ray background, the electronic threshold was set in the arrow position. Figure 1b) shows the typical amplitude spectra obtained for all counters during the cell heat production period.

The absolute efficiency (²) was measured by placing the Am-Be source, without moderator, 8 m away from the detector centre. The values obtained are reported in table I.

In the following, two series of data taken in different periods are presented:

- i) detector *C2* placed near the cell A and *C1* far away,
- ii) all detectors placed near the cell A.

Initially (point i)), while cell A was already in the *excited state*, detector *C2* was placed 39 cm away from the cell centre, while detector *C1* was placed about 10 m away. For each detector the number of pulses was summed and recorded every ten minutes.

In figs. 2a) and b) the counting rate *versus* time is reported for detector *C2* and *C1*, respectively. Both plots refer to the same short time period (12.00 h of 11 March 1995) because an electric breakdown occurred during the week-end caused a loss of data. Two effects can be observed:

- a) the counting rate measured near the cell is greater than the neutron cosmic-ray background.
- b) the *C2* counting rate distribution is very different from the one expected, *i.e.* Poisson statistics.

Such large deviations from the mean value occurred during a brief period for which the power emitted from the cell A had a spontaneous increase (of the order of 10 W) and several input power reductions were needed to keep the working point temperature as constant as possible.

The cosmic-ray *C1* counting rate and efficiencies of both detectors were utilized for obtaining the *C2* background. After subtraction of such background, we obtained

$$(1) \quad N'(C2) = 252 \pm 3 \text{ counts/10 minutes.}$$

Successively, (point ii), see fig. 3 for the experimental layout) detector *C1* was moved and placed closer to the cell (44 cm away from its centre). Further the *C3* detector, not yet cadmium shielded at that time, was added and placed 28 cm away from the cell centre. Four movable neutron shields (5.7 cm of polythene and 1 cm of powdered boric acid) were placed around the apparatus for safety reasons. The cell activity was monitored for a long time period by utilizing the *C1*, *C2* and *C3* detectors. In fig. 4 the counting rate *versus* time for detector *C2* is shown. It is worthwhile observing the big difference with fig. 2a) which refers to a great activity period of the cell.

Later on, the cell *normal* (not *excited*) state was restored by decreasing the Ni temperature below 540 K. After this the same input power as before was supplied to the cell (in order to avoid a possible influence due to load changes), the radiation shields were left in place and the detectors were employed to measure the cosmic neutron background.

In table II the mean counting rates obtained in period ii) (10 minutes cumulation time) N_{C1}^* , N_{C2}^* , N_{C3}^* are reported for different runs (for detector *C3* only the measurements after shielding it with cadmium are reported).

(²) Defined as the ratio between the number of pulses recorded by one counter set within its moderator and the number of neutrons emitted by the source.

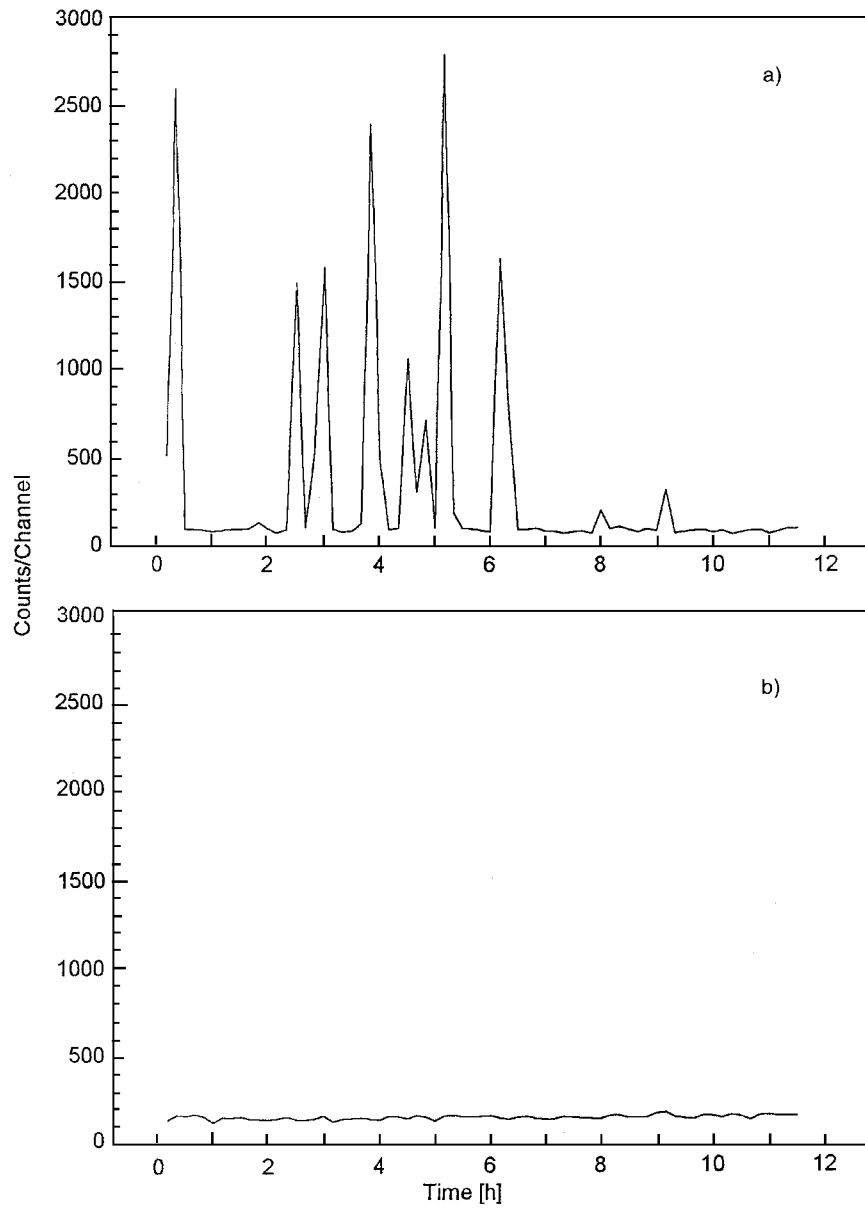


Fig. 2. – a) Counting rate of detector *C2* placed 39 cm away from the cell (11 March 1995). Each point represents the number of pulses recorded in 10 minutes. b) Counting rate of detector *C1* placed 10 m away from the cell (laboratory background). Each point represents the number of pulses recorded in 10 minutes.

The neutron mean emission rate from cell A was obtained, for each detector, as follows.

For a source, the neutron counting rate can be expressed as

$$(2) \quad N = S \frac{\Omega}{4\pi} \epsilon,$$

TABLE II. – Mean counting rate $N_{C_1}^*$, $N_{C_2}^*$ and $N_{C_3}^*$ expressed in counts/10 minutes.

Run (1995)	$N_{C_1}^*$	$N_{C_2}^*$	$N_{C_3}^*$	Cell status
April 26–28	87.54 ± 0.54	73.32 ± 0.55	–	excited
May 4–9	82.02 ± 0.33	69.31 ± 0.31	–	excited
May 11–15	89.58 ± 0.43	75.42 ± 0.39	–	excited
June 19–26	84.60 ± 0.30	71.79 ± 0.27	52.48 ± 0.23	excited
June 26–29	86.18 ± 0.44	74.04 ± 0.41	56.32 ± 0.35	excited
July 1–6	88.28 ± 0.18	72.92 ± 0.16	52.60 ± 0.14	excited
April–July	86.76 ± 0.12	72.59 ± 0.11	52.97 ± 0.11	excited
August 7–9	77.98 ± 0.52	61.06 ± 0.46	46.99 ± 0.41	normal

where S is the source strength, Ω the solid angle and ϵ the mean efficiency of the detector

$$(3) \quad \epsilon = \int_E \epsilon(E) f(E) dE.$$

In eq. (3) $f(E)$ is the spectral function of the neutrons from the source (see ref. [5] for Am-Be).

In a similar way the cell neutron counting rate can be expressed as

$$(4) \quad N' = S' \frac{\Omega'}{4\pi} \epsilon',$$

where N' is obtained from N^* by background subtraction.

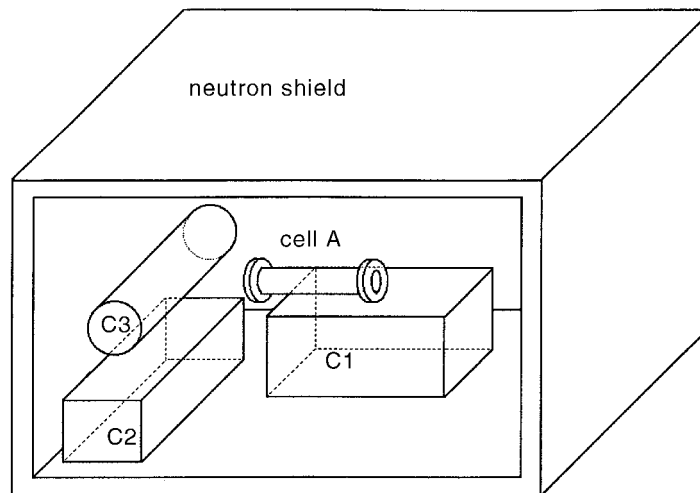


Fig. 3. – Schematic drawing of detectors C_1 , C_2 and C_3 placed around the cell A.

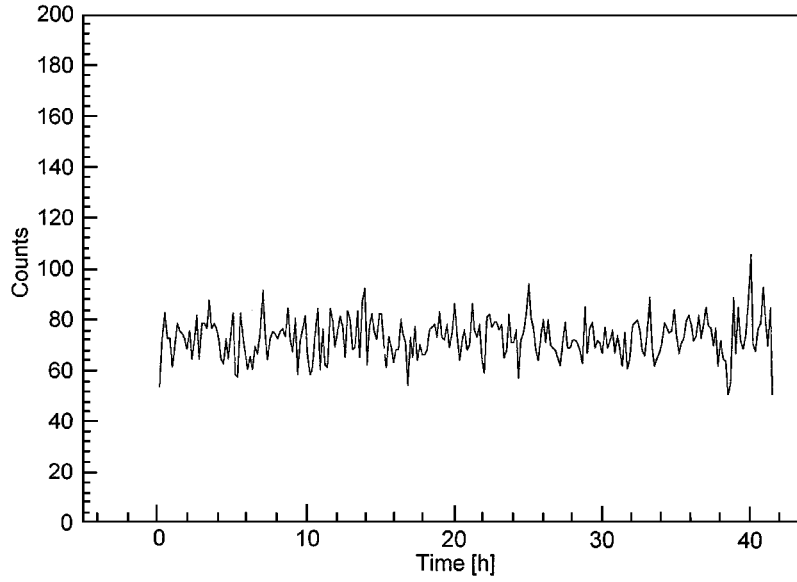


Fig. 4. – Counting rate of detector *C2* placed 39 cm away from the cell (42 hours in the period 19–26 June 1995). Each point represents the number of pulses recorded in 10 minutes.

By assuming that the mean efficiency ϵ' is of the same order as ϵ , one obtains the neutron intensity from the cell

$$(5) \quad S' = S \frac{N'}{N} \frac{\Omega}{\Omega'} \frac{\epsilon}{\epsilon'} \approx S \frac{N'}{N} \frac{\Omega}{\Omega'}.$$

In a pointlike source approximation, S' can be expressed as

$$(6) \quad S' \approx S \frac{N'}{N} \frac{r'^2}{r^2},$$

with an obvious meaning for the symbols.

By inserting in the previous formulae our experimental data, after subtracting background, the neutron mean emission rate S' from the cell A in the two different periods can be evaluated as follows:

period i)

$$(7) \quad S'(C2) \approx 110 \text{ neutrons/s},$$

period ii)

$$(8) \quad S'(C1) \approx 5 \text{ neutrons/s}, \quad S'(C2) \approx 5 \text{ neutrons/s}, \quad S'(C3) \approx 2 \text{ neutrons/s}.$$

The values reported above are obtained by considering all counts as due to neutrons coming directly from the source. Since the detectors were placed in different positions with respect to the shields (see fig. 3) the contribution of the scattered neutrons is

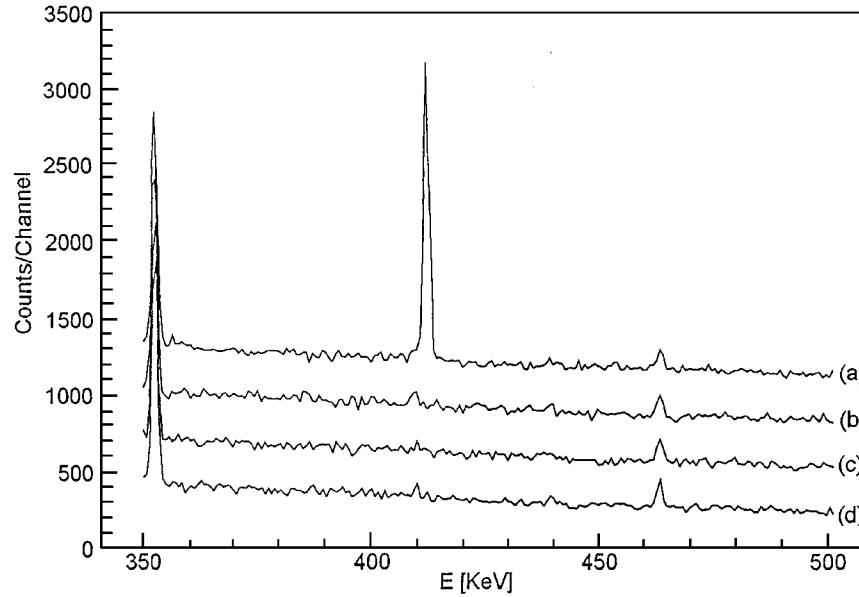


Fig. 5. – Gamma-ray spectra in the 350–500 keV region obtained with a germanium detector for: (a) gold sheet after the activation for 12 days on cell A; (b) gold sheet after the same exposition time to cosmic rays 10 m away from the cell; (c) gold sheet before the activation on the cell; (d) laboratory background.

clearly different. This could be the reason why the counting rates (8) of the detectors are different.

3. – Gold activation

The second method used in the present measurement for neutron detection consists in the activation by (n, γ) reactions. Few elements, as is well known, have a high thermal cross-section for neutron capture. Among these, gold also has the characteristic of having some resonance peaks at energies higher than the thermal one.

^{197}Au transmutes in ^{198}Au by the reaction $^{197}\text{Au}(n, \gamma)^{198}\text{Au}$. The latter decays with a 2.7 day halflife according to the process



in the $^{198}\text{Hg}^*$ (411.8) level with a 99% branching ratio. The $^{198}\text{Hg}^*$ decays to the ground state by emission of a 411.8 keV gamma-ray (E2 transition) [6].

We used a paraffin box ($16 \times 22 \times 5 \text{ cm}^3$) to thermalize neutrons. The box, containing inside it a $5.1 \times 2.4 \times 0.06 \text{ cm}^3$ gold sheet was placed near the cell for 12 days (3–15 March 1995). The gamma-rays emitted in the $^{198}\text{Hg}^*$ decay were detected by a germanium detector (ORTEC mod. GEM-10175 and computer card acquisition SILENA mod. 9308). Curve (a) of fig. 5 shows the recorded spectrum in the 350–500 keV region. Curve (d) represents the laboratory background in the same energy interval, while curve (c) shows the spectrum obtained on placing the same gold sheet on the germanium detector before activation. In order to rule out a cosmic-ray neutron origin for the observed signal, the

gold contained in the paraffin box was left for 12 days at 10 m from the cell. The gamma spectrum obtained after such exposition is reported in curve (b). The counting time was the same (12000 s) for all curves, which are presented for the sake of clarity shifted upwards with respect to curve (d).

Let S and R be, respectively, the number of neutrons emitted per second from a source and the number of gold nuclei activated per second inside the box, then

$$(10) \quad R = S \frac{\Omega_M}{4\pi} \epsilon_a,$$

where Ω_M is the solid angle between source and moderator and ϵ_a the activation efficiency, which depends on the neutron energy spectrum and the box geometry.

If S is constant in time, the number of ^{198}Au nuclei in the sheet depends on the exposition time t according to

$$(11) \quad N_{\text{Au}}(t) = \frac{R}{\lambda} (1 - e^{-\lambda t}),$$

where λ is the inverse of the mean life.

The number of gamma recorded from the germanium detector at a time t_2 after a source exposition of t_1 seconds, is

$$(12) \quad N_\gamma = \frac{S}{\lambda} \frac{\Omega_M}{4\pi} \epsilon_a (1 - e^{-\lambda t_1}) \frac{\Omega_D}{4\pi} \epsilon_R (1 - e^{-\lambda t_2}),$$

where Ω_D is the solid angle between the gold sheet and the detector and ϵ_R the germanium efficiency at 411 keV.

In order to deduce the neutron intensity from the cell, we placed the gold sheet contained in the paraffin box 10 cm away from the known Am-Be neutron source for 9.5 hours. The gamma spectrum recorded from the germanium detector in 12000 s after such an exposition is shown in fig. 6.

A Monte Carlo simulation [7] showed that, for our moderator, the gold capture rate is almost constant (within a factor two) in a neutron energy range up to 10 MeV. On this basis we can assume that the efficiency ϵ_a is the same for neutrons emitted from the Am-Be source and from the cell. Thus the following relation is obtained:

$$(13) \quad \frac{S'}{S} \approx \frac{N'_\gamma}{N_\gamma} \frac{\Omega_M}{\Omega'_M} f(t_1, t_2, t'_1, t'_2),$$

where the primed variables refer to the cell, the unprimed ones to the Am-Be source and the value of the function f depends on the measurement times.

After background subtraction we obtained for the number of gamma-rays recorded

$$(14) \quad N'_\gamma = 4004 \pm 90,$$

$$(15) \quad N_\gamma = 5144 \pm 96.$$

From our experimental data it is possible to estimate the order of magnitude of the intensity of the cell as a source

$$(16) \quad S' \approx 6000 \text{ neutrons/s.}$$

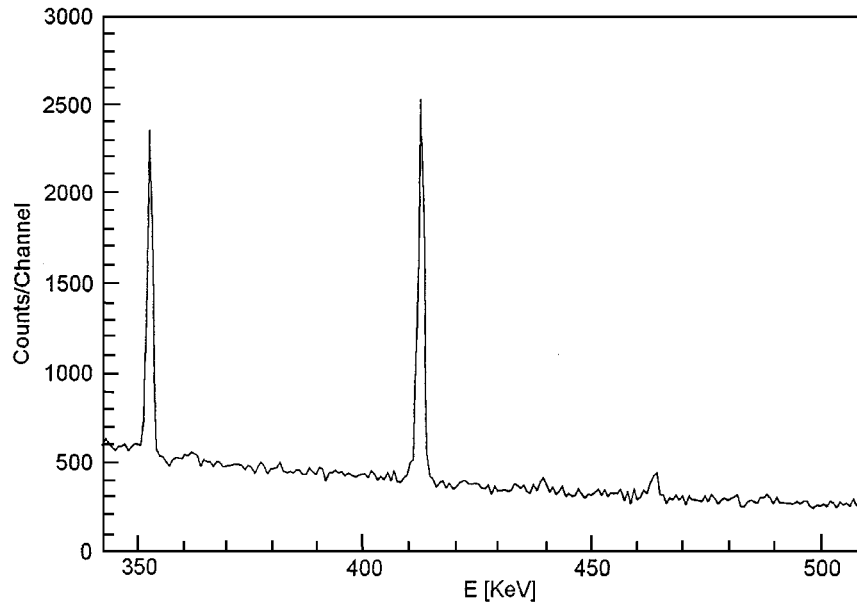


Fig. 6. – Gamma-ray spectra in the 350–500 keV region obtained with a germanium detector for the same gold sheet, previously utilized on the cell, after the activation on an Am-Be source. The exposition time was 9.5 hours.

The method used (on comparison with a source of known strength) also allows one to avoid all complications connected to the flux depletion due to the thick gold sheet.

The estimate reported in eq. (16) differs by a factor of about 50 with that obtained in measurements partially overlapping in time from the neutron detectors (eq. (7)). This may well be due to the way neutrons are emitted: bursts instead of a homogeneous flux, as shown in fig. 2a) which can imply pile-up and dead-time effects in the neutron counter chain. Furthermore in the period of time in which gold was activated, the neutron intensity was exceptionally high in measurements partially overlapping in time. Later on, in the period ii) (April–July 1995) when the detector measurements were performed (see table II and fig. 4 which is to be compared with fig. 2a)) the neutron intensity was lower. Thus, the apparent disagreement between eqs. (8) and (16) depends on the varying neutron intensity. In fact during this period it was not possible to obtain a detectable gold activation.

As a test of internal consistency of the data shown in fig. 5, the neutron mean flux from the cell through the gold sheet was estimated. Starting from eq. (16), neglecting the flux depletion, and assuming a pointlike source, one has

$$(17) \quad \phi' \approx 10 \text{ neutrons/cm}^2\text{s}.$$

On the other hand, the cosmic-ray neutron flux measured at 200 g/cm² from the top of the atmosphere [8] allows one to estimate a neutron flux

$$(18) \quad \phi_c \approx 0.01 \text{ neutrons/cm}^2\text{s}$$

for Siena (450 m over sea level).

The value of the ratio

$$(19) \quad \frac{\phi'}{\phi_c} \approx 10^3$$

agrees with the fact that no activation was observed when the gold sheet was exposed to cosmic rays.

4. – Discussion and conclusions

As already pointed out, the search for direct signals of nuclear reactions was stimulated by the need to explain the large energy production in our cells. The neutron detection here reported supports the hypothesis that nuclear reactions occur during the cell activity.

On the other hand, we note that the neutron flux is not constant in time, changing by orders of magnitude as proved by measurements performed with two different methods (gold activation and He³ counters). In fact we underline that in period i) we had simultaneously high counting rates and gold activation while in period ii) we had a counting rate slightly higher than the background and no gold activation. Moreover experimental data support the hypothesis that the neutron flux is correlated with the power excess rate increase instead of the power excess level.

Assuming that each reaction releases a mean energy of the order of 1 MeV, one would obtain about 2×10^{14} reactions/s when the maximum neutron flux was observed. From our maximum observed emission (eq. (16)) it is then possible to estimate that about one reaction with neutron emission occurs every 10^{11} reactions. This figure appears too small to be acceptable within the current nuclear physics knowledge.

Work is in progress in order to identify the main nuclear chains.

* * *

We wish to thank Profs. T. BRESSANI, P. CAMMAROTA, A. DEL CORSO, C. STREMMENOS, A. TROMBETTI, and Drs. E. FANARA and G. MAGRO for helpful suggestions and discussions. Special thanks are also due to Prof. R. HABEL for its collaboration in the initial phase of the experiment.

REFERENCES

- [1] FOCARDI S., HABEL R. and PIANTELLI F., *Nuovo Cimento A*, **107** (1994) 163.
- [2] FOCARDI S., GABBANI V., MONTALBANO V., PIANTELLI F. and VERONESI S., *Nuovo Cimento A*, **111** (1998) 1233.
- [3] FOCARDI S., GABBANI V., HABEL R., MONTALBANO V., PIANTELLI F. and VERONESI S., *Status of cold fusion in Italy, IV - Proceedings of Siena Workshop, Siena, 24-25 March 1995*, unpublished.
- [4] BATCHELOR R., AVES R. and SKYRME T. H. R., *Rev. Sci. Instrum.*, **26** (1955) 1037.
- [5] LORCH E. A., *Int. Appl. Rad. Isotop.*, **24** (1973) 585.
- [6] LEDERER C. M., HOLLANDER J. M. and PERLMAN I., *Table of Isotopes* (John Wiley and Sons, New York) 1967, p. 384.
- [7] STUPAZZONI L., thesis, Bologna University (1995).
- [8] BOELLA G., DEGLI ANTONI G., DILWORTH C., GIANNELLI G., ROCCA E., SCARSI L. and SHAPIRO D., *Nuovo Cimento*, **29** (1963) 103.